2024

Conservation impact assessment and SAR forest cover mapping in the Colombian Andes

BOSTON UNIVERSITY

GRADUATE SCHOOL OF ARTS AND SCIENCES

Thesis

CONSERVATION IMPACT ASSESSMENT AND SAR FOREST COVER MAPPING IN THE COLOMBIAN ANDES

by

EMILY DAWSON FRENCH

B.A., Middlebury College, 2019

Submitted in partial fulfillment of the

requirements for the degree of

Master of Arts

2024

Approved by

First Reader

Christoph Nolte, Ph.D.
Professor of Earth and Environment

Second Reader

Paulo Arévalo, Ph.D.
Research Scientist Center for Remote Sensing

Third Reader

Curtis Woodcock, Ph.D.
Professor of Earth and Environment

Fourth Reader

Robert Kaufmann, Ph.D.
Professor of Earth and Environment

ACKNOWLEDGEMENTS

First, thanks to Christoph Nolte for giving me the opportunity to attend BU, for sharing your expertise, and for being a kind and enthusiastic advisor. Also, thank you to Paulo Arévalo for your encouragement and the many hours of Google Earth Engine and remote sensing support. I have learned so much from working with you both.

I would also like to thank Curtis Woodcock and Robert Kaufmann for their dedication to teaching and working with students. In particular, I appreciate you taking the time to give feedback as members of my thesis committee. Thanks also to Ana Reboredo Segovia for laying much of the groundwork for Chapter One and for sharing your expertise so generously.

Finally, I acknowledge that this work would not be possible without the contribution of the many other researchers who have shared code, published educational materials and taken the time to make their work accessible.

CONSERVATION IMPACT ASSESSMENT AND SAR FOREST COVER MAPPING IN THE COLOMBIAN ANDES

EMILY DAWSON FRENCH

ABSTRACT

This thesis addresses research questions from two distinct yet complementary fields—conservation science and remote sensing—through a case study in the Colombian Andes. In Chapter One, we explore the impact on forest cover of the largest and longest-running public land acquisition (PLA) program in the tropics between 2000 and 2021. Using matching and Difference-in-Differences with multiple time periods we find that as of 2021 there has been a 3.5% increase in forest cover on protected parcels and that impact increases for at least 10 to 12 years post-treatment. We also find that impact varies significantly by factors like slope, accessibility, and department. In Chapter Two, we attempt to improve the forest cover data used in Chapter One by integrating synthetic aperture radar (SAR) observations from Sentinel-1 for areas where persistent cloud cover precludes the use of optical data. We find encouraging evidence to suggest that SAR data can be used with the continuous change detection and classification algorithm to detect forest change in topographically-complex regions, but conclude that accuracy improvements and widespread workflow adoption are dependent on the accessibility of high resolution digital elevation models and improved radiometric terrain correction for Google Earth Engine.

TABLE OF CONTENTS

LIST OF TABLES

LIST OF FIGURES

LIST OF ABBREVIATIONS

ATT	Average Treatment effect on the Treated
CCDC	Continuous Change Detection and Classification
DEM	Digital Elevation Model
DiD	Difference-in-Differences
GEE	Google Earth Engine
GRD	Ground Range Detected
IGAC	Instituto Geográfico Agustín Codazzi
IW	Interferometric Wide
PA	Protected Area
PLA	Public Land Acquisition
RADD	Radar for Detecting Deforestation
RGB	Red Green Blue
RMSE	Root Mean Square Error
RTC	Radiometric Terrain Correction
SAR	Synthetic Aperture Radar
SRTM	Shuttle Radar Topography Mission
VH	Vertical Horizontal
VV	Vertical Vertical

CHAPTER 1: Evaluating the Impact of Public Land Acquisitions on Forest Cover in the Colombian Andes

Authors: Emily D. French, Christoph Nolte

1.1. Introduction

The Tropical Andes is one of the most biodiverse regions in the world. Forests here provide key ecosystem services including carbon sequestration and water source protection. Despite significant conservation spending—totaling around 50 million USD annually in Colombia alone (Waldron, A., et al., 2013)—this region still experiences high rates of forest degradation and deforestation and ranks as one of the most threatened areas of the tropics (Ritchie, 2021; CEPF, 2015). For decisionmakers, understanding the impact of consevation instruments is central to building robust, cost-effective, conservation networks that protect both biodiveristy and human well-being. One of the most widespread and well-studied conservation instruments are protected areas (PAs). Despite their popularity, PAs can be ineffective without adequate funding and enforcement. Furthermore, they pose equity concerns when communities lose access to land without compensation. This dynamic is particularly problematic in Colombia given a high degree of land tenure informality and internal displacement due to violent conflict (Few et al., 2021). In response, direct incentive programs like public land acquisitions (PLAs) which compensate landowners for ceding land-use rights have become an increasingly popular alternative or even complement to traditional PAs. While PLAs are well-studied in wealthy countries, there is limited evidence about the effectiveness of PLAs in low and middle-income countries. In this context, evaluating the Colombian PLA network will

provide valuable insight for decisionmakers not only in Colombia but also in the many countries where the impact of direct incentive programs has not yet been studied.

Colombia presents a rich empirical context to study PLAs. Since 1993, Article 111 of law 99 mandates that all Colombian departments spend 1% of their annual income on land acquisitions for water conservation (Fondo Acción, 2017). Previous work assesses the scale and extent of PLAs in Colombia as well as the impact of PLAs on forest cover in Eastern Antioquia (Reboredo Segovia et al., 2022; Reboredo Segovia et al., in progress). This study leverages the unique, spatially explicit PLA dataset compiled by Reboredo Segovia et al. to assess the impact of PLAs on forest cover across 18 Colombian departments between 2000 and 2021. Specifically, we ask: 1) How do characteristics that affect the probability of deforestation differ between PLAs and unprotected areas? 2) What is the impact of PLAs on forest cover? 3) How does this impact vary based on factors like slope, accessibility, department, and protection status?

1.2. Methods

1.2.1. Study Area

In this study, we consider PLAs across the Colombian Andes which we define as the maximum extent of three ecoregions: Northern Andean Montane Forests, Northern Andean Parámo, and Tumbesian-Andean Valleys Dry Forests (Olson et al., 2001). Our study area includes the 314 Colombian municipalities that have at least one PLA established between 2000 and 2019 and their immediate municipal abutters (Figure 1.1).

We estimate that the background deforestation rate for this area is approximately 0.1% between 1997 and 2021.

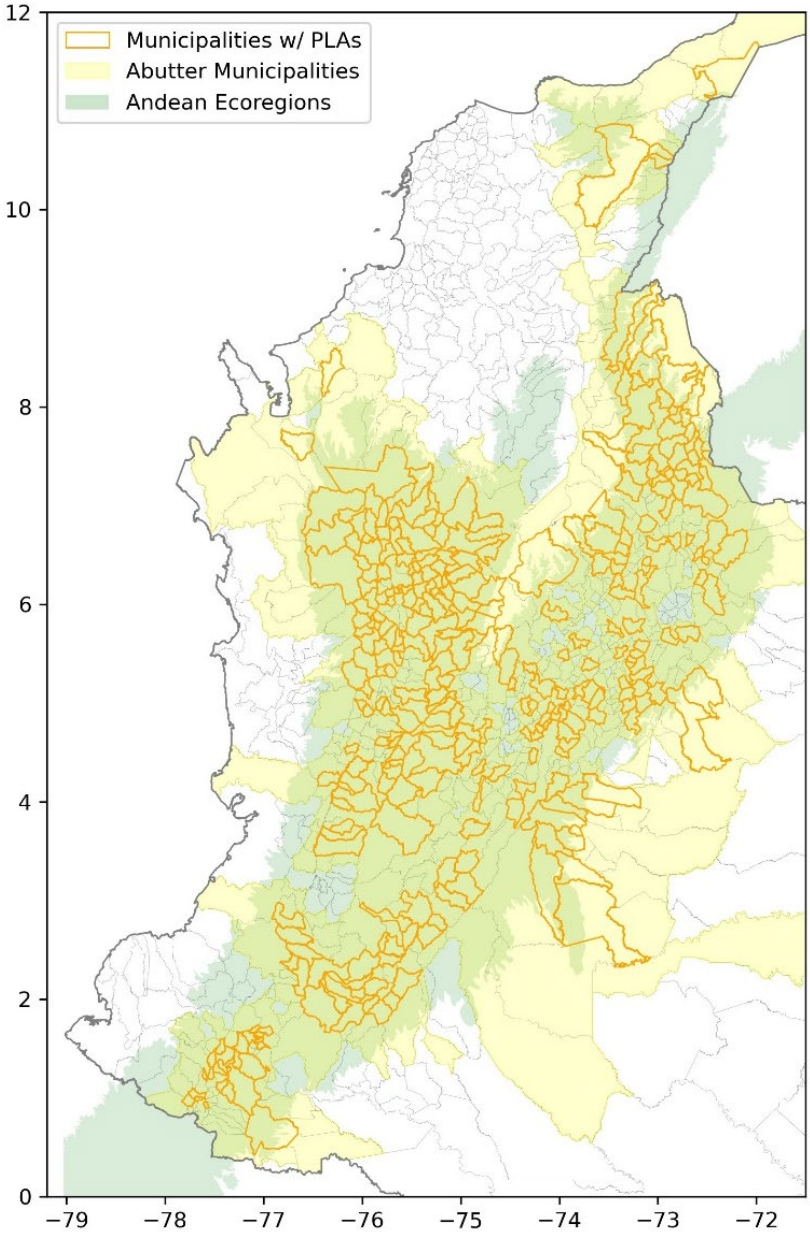

Figure 1.1. Study area including Colombian municipalities with a PLA established between 2000 and 2019 (orange) and their neighbors (yellow).

1.2.2. Forest Cover Data

Our primary unit of analysis is percent forest cover at the parcel level. Percent forest cover was derived from annual land cover maps for the years 1997 to 2021 (Bullock and Arévalo, in progress). These maps were generated using an ensemble approach that applied a stacking generalization protocol (Healey et al. 2018) to combine the outputs of two change detection algorithms, Continuous Change Detection and Classification and LandTrendr, and one forest change product (Zhu & Woodcock, 2014; Kennedy et al., 2014; Hansen et al., 2013).

1.2.3. Parcel and PLA Data

Parcel data for all departments was obtained from the Colombian cadaster (IGAC) data portal with the exception of Antioquia which has its own geodatabase. The PLA dataset used in this study was compiled with data from 24 regional environmental agencies, 14 departments, and 107 municipalities. For a more comprehensive description of PLA data collection see Reboredo Segovia et al. 2022. We compiled our treatment dataset by selecting cadaster parcels that share more than 80% of their area with a PLA boundary. Note that because cadaster parcel boundaries were used to compile the original PLA dataset, in many cases PLA and cadaster geometries were equivalent. Due to the temporal limitations of the land cover data, we limit our analysis to PLAs established between 2000 and 2019 to avoid errors associated with measuring treatment effect over a very narrow window (less than three years). Given our imposed temporal limitations as well as missing spatial and treatment date information we were only able to measure the impact for 2,327 of the 4,462 (53%) PLAs from the original dataset. To prepare parcels

for matching and difference in differences, we performed zonal statistics to calculate elevation, slope, accessibility, distance to water, area, and yearly percent forest cover for each parcel. We also identified parcels inside Indigenous Reserves and National and Regional Parks.

1.2.4. Matching

To estimate the causal impact of PLAs on forest cover, we used matching followed by difference in differences (DiD) with multiple time periods. The goal of matching is to control for observable confounding variables so that the forest cover trends for matched parcels mirror the counterfactual outcome for treated parcels. In other words, the forest cover trends for control parcels should be the same as those that would have been observed on treated parcels had they not been treated. Selected matching variables include percent forest cover on the year prior to treatment, slope, elevation, measures of accessibility including travel time to cities and night lights, distance to water, parcel area, and whether or not the parcel is inside an existing protected area. See Table 1.1 for a complete description of matching variables. DiD with multiple time periods allows for not-yet-treated control observations (observations that eventually receive treatment but are untreated for some portion of the study period). To increase the chances of finding a quality match for as many treatment parcels as possible, we allow treated parcels to match with either never-treated or not-yet-treated parcels. We matched without replacement following a novel protocol developed by Reboredo Segovia et al. for their work comparing the impact of PLAs and another direct incentive program, payments for ecosystem services, on forest cover in Eastern Antioquia (Reboredo Segovia et al., in

progress; Nolte et al., 2019). Of 2,327 PLAs established between 2000 and 2019 with valid spatial and treatment date information, 2,297 were successfully matched. 30 PLAs were dropped when a match could not be found within 1 standard deviation of the treatment parcel value for one or more covariates. After matching, we plotted the density distribution of covariates for never treated parcels, treated parcels, and matched controls (Figure 1.2). These plots show that we were successfully able to control for the selected observable covariates. They also allow us to investigate how characteristics that affect the probability of deforestation differ between PLAs and unprotected areas (Q1).

Table 1.1. Selected matching variables (covariates)

Variable	**Source**	**Year Used**	**Resolution**	**Justification**
% Forest Cover on Year Prior to Treatment	Bullock and Arévalo (in progress)	1997 - 2021	30 m	Affects potential forest change and treatment selection.
Elevation	Japan Areospace Exploration Agency (2021)		30 m	Can influence deforestation pressure.
Slope	Derived from elevation		30 m	Areas with high slope are less arable and may have lower deforestation pressure. Can affect treatment selection because steep slopes are a priority for water source protection.
Travel Time to Cities (access)	Nelson (2008)	2000	30 arc seconds	Accessible areas have higher deforestation pressure. Remote parcels may be more likely to be selected for treatment if other economic activity is limited by inaccessibility.

Night Lights (access)	Small et al. (2011)	2001-2013 (avg.)		Similar to travel time but includes smaller towns and rural electrification patterns.
Distance to Water	Derived from elevation		30 m	Areas with limited access to water may have lower deforestation pressure. Parcel may be more likely to be selected for treatment if other economic activity is limited.
Parcel Area (log transform)	GIS calculation		Vector	Determines the yearly level of observable deforestation due to 30m resolution of land cover data.
PA Category	RUNAP (2023); Agencia Nacional de Tierras (2024)		Vector	PA categories have varying restrictions and enforcement that may influence deforestation and regrowth dynamics.
Municipality and Abutters	Departamento Administrativo Nacional de Estadística (2005)		Vector	Accounts for unobserved regional socioeconomic differences that influence deforestation, enforcement, and enrollment.

1.2.5. Difference-in-Differences with Multiple Time Periods

Recent work by Callaway and Sant'Anna highlights how the canonical two-way fixed effects DiD design can yield biased estimates when interventions have staggered implementation (i.e. are implemented over multiple years) (2021). To estimate the impact of PLAs established over many years we use Callaway and Sant'Anna's DiD with multiple time periods approach in R which works by calculating an individual average treatment effect on the treated (ATT) for each treatment group (g) at each time (t). The overall treatment effect on the treated is the weighted average of all individual group-time

ATTs where weights are proportional to the size of each group-time cohort. To assess the impact of PLAs on forest cover (Q2) we calculate the overall ATT as well as the ATT aggregated by calendar year, treatment group and exposure length. Aggregating by calendar year, treatment group and exposure length allows us to assess how PLAs impact forest cover over time. We also ran subgroup analyses to assess how forest cover impact varies based on factors like slope, accessibility, department, and protection status (Q3). Due to reduced sample sizes, subgroup results are limited to the overall treatment effect for each subgroup.

1.3. Results

1.3.1. Density Distributions

We plotted density distributions to assess to what extent characteristics that affect the probability of deforestation differ between PLAs and unprotected areas (Figure 1.2). For elevation, we found that treated parcels tend to be at higher elevations (2182 m average) than never-treated parcels (1382 m average) similarly, never-treated parcels tend to have flatter slopes (9% average) when compared to PLAs (20% average). It follows that PLAs are also generally further from water and tend to be more remote (3.6 hours average) than never-treated parcels (1.9 hours average). Finally, we found that PLAs are also, on average, larger than never-treated parcels which is unsurprising given that PLAs are rarely located in urban areas which tend to have the smallest parcel sizes.

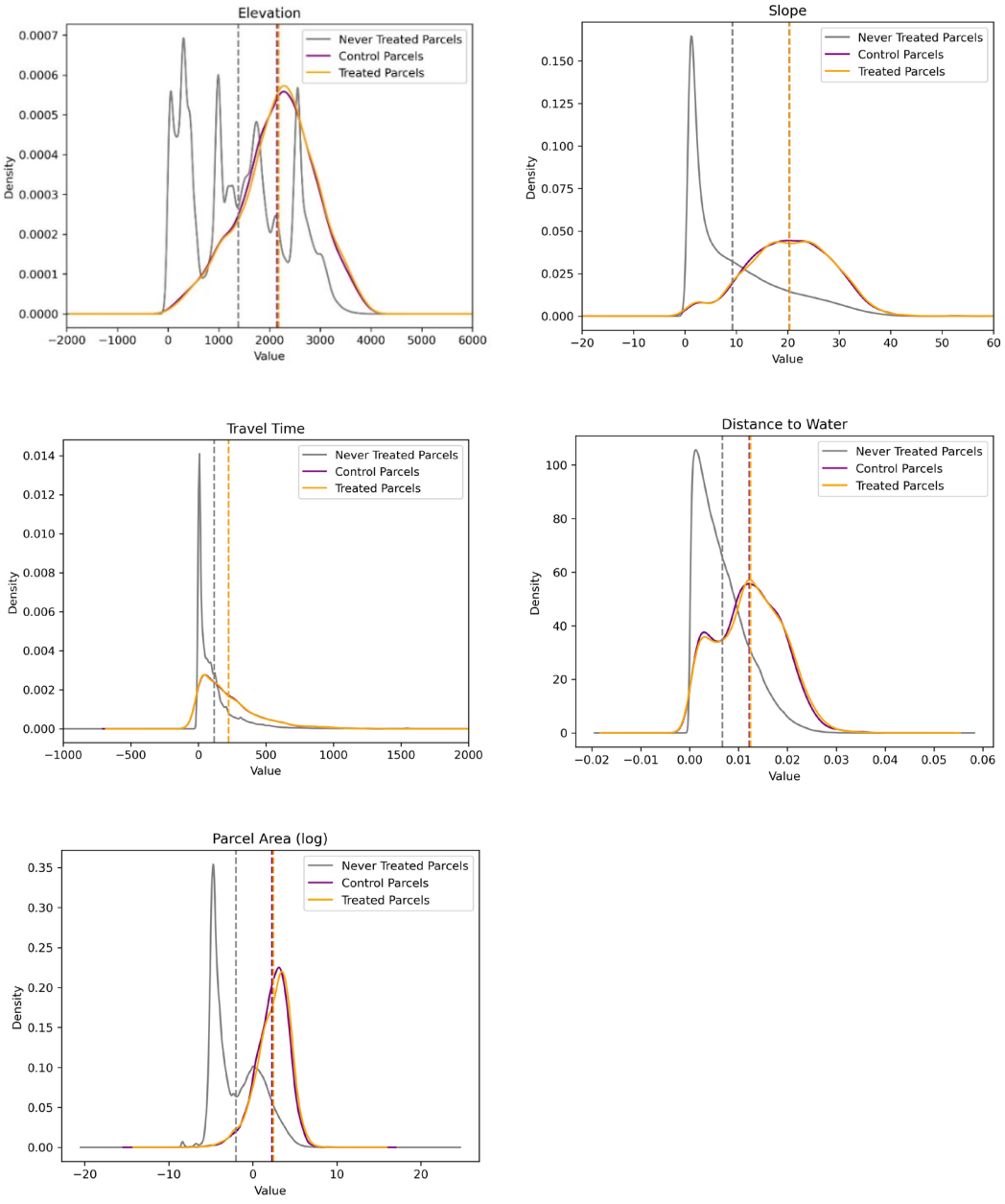

Figure 1.2. Distribution of covariates that impact percent forest cover for never treated parcels (grey), treated parcels (orange), and their matched controls (purple).

1.3.2. Overall Impact

We estimate an overall ATT of 2.1% across all PLAs. In other words, across all treatment groups and years the average impact of PLAs on forest cover is a 2.1% increase when compared to matched controls. Figure 3 shows the overall ATT (red) compared to calendar year estimates. Calendar year estimates show a steady increase in treatment effect every year from 2000 to 2021. Estimates become more robust as more PLAs are treated. The cumulative impact of PLAs on forest cover is an estimated 3.5% increase as of 2021. We also calculated ATT by treatment group (ie. the year a PLA was protected) and found that PLAs protected in 2003 and 2006 have the highest average percent impact, 3.4% (CI +/- 2.6%) and 4.4% (CI +/- 1.6%), respectively (Figure 1.4). The anomalously low ATT for PLAs established in 2002 warrants further investigation. Aggregating ATT by exposure length shows that the impact of intervention increases over time for the first 10 to 12 years (Figure 1.5). A previous study on PLAs in Eastern Antioquia suggests that forest regrowth may play an important role in this dynamic (Reboredo Segovia et al., in progress). By year 17, estimates are no longer statistically significant due to small sample sizes and a general pattern of lessening impact at the end of the study period.

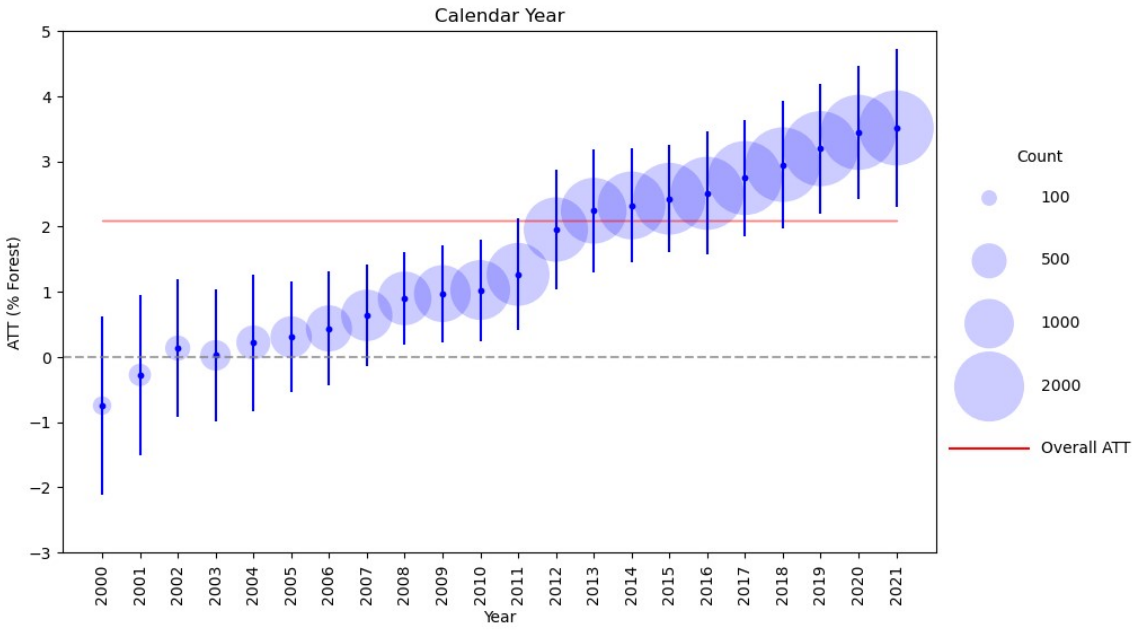

Figure 1.3. ATTs averaged by calendar year. Error bars show the 95% confidence interval for the impact estimate.

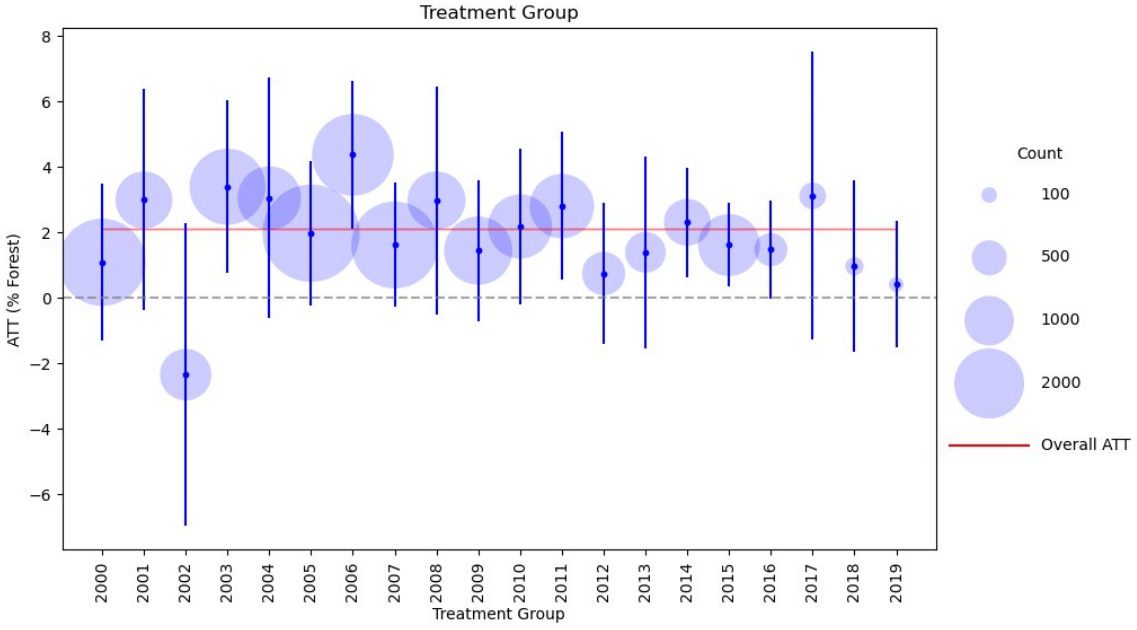

Figure 1.4. ATTs averaged by treatment group. Error bars show the 95% confidence interval for the impact estimate.

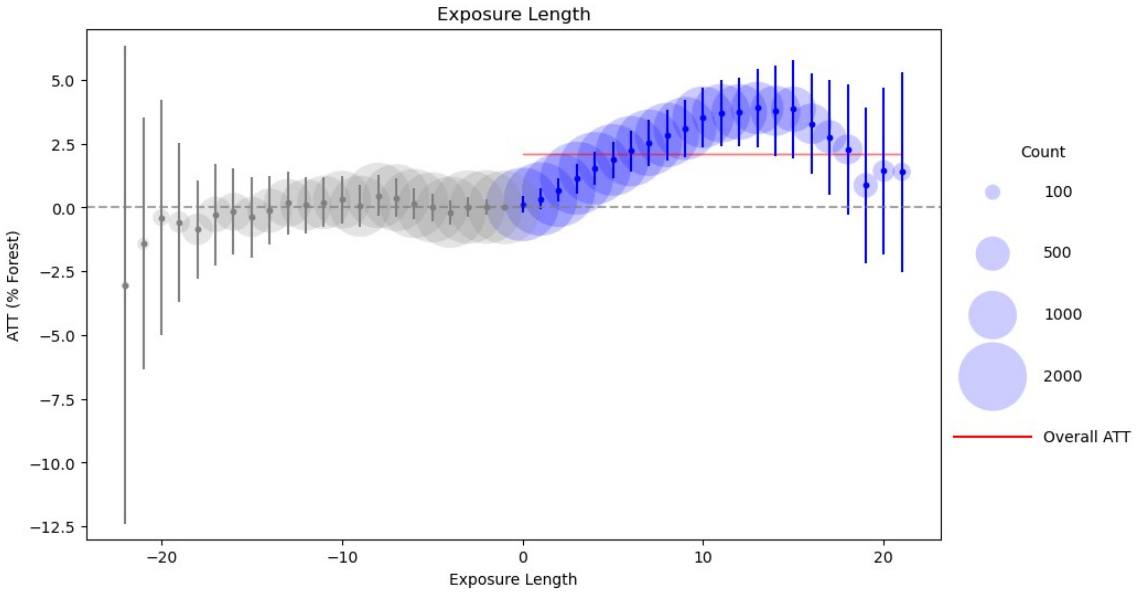

Figure 1.5. ATTs averaged by exposure length (number of years) pre (grey) and post (blue) treatment. Error bars show the 95% confidence interval for the impact estimate.

1.3.3. Subgroup Analysis

Slope subgroup analysis revealed that PLAs with moderate slope, between 15% and 30%, have a larger impact on percent forest cover than PLAs with relatively flat slopes, below 15%, or steep slopes, above 30%. For all groups except PLAs with the steepest slopes, we found a statistically significat positive impact on forest cover. This is likely indicative of steep slopes having lower deforestation pressure which, if true, would cause the total avoided deforestation to decrease as slope increases. Travel time subgroup anaysis reveals a similar dyanmic. In this case, all subgroups show a statistically significant positive impact on forest cover but the impact is much larger for PLAs with travel times between 0 and 2 hours (2.7%) and between 2 and 4 hours (3.1%) than it is for the most remote PLAs (0.8%). We also find that PLAs inside PAs (including national parks, regional parks, and indigenous reserves) have a lower overall ATT than

unprotected PAs, 2.15% (CIs +/- 0.5%) and 1.2% (CIs +/- 2%), respectively. Considering ATT estimates have similar standard deviations, 2.16 for PLAs outiside of PAs and 1.96 for PLAs inside of PAs we conclude that the small sample size for protected PLAs (45) is the primary cause of the large and ultimately non-significant confidence intervals for this estimate. Regardless, comparions for these two groups cannot be made with a high degree of confidence. Finally, department subgroup analysis shows that the impact of PLAs varies significatly by subgroup. Of the 18 departments with at least one PLA, 8 have a statistically significant positive ATT for percent forest cover. Of the departments with non-significant ATTs several have an estimated impact below 1% including Cauca, Cundinamarca, Huila, Putumayo, Santander, and Valle del Cauca.

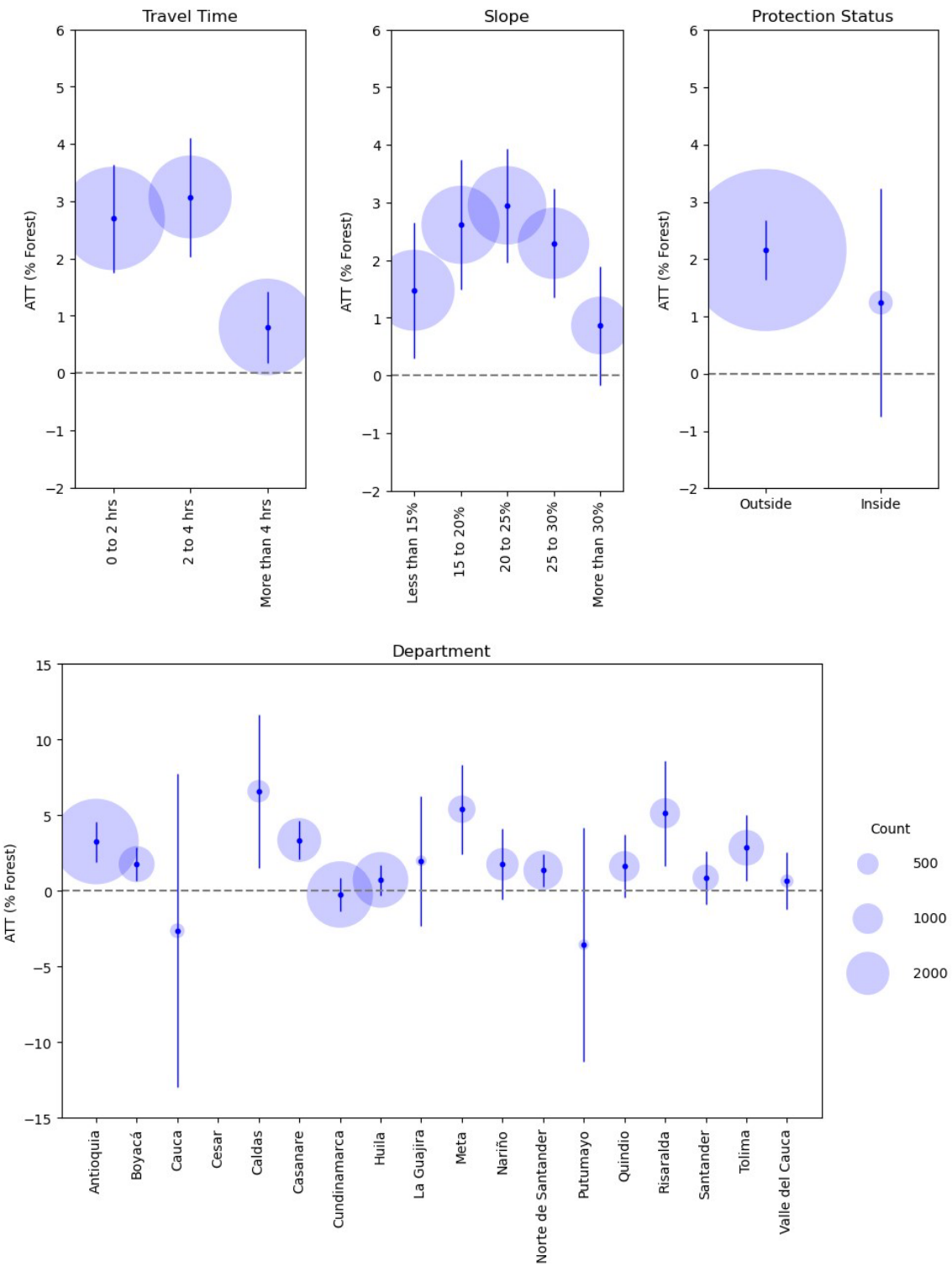

Figure 1.6. Overall ATT for subgroups. Error bars show the 95% confidence interval for the impact estimate.

1.4. Discussion

1.4.1. Subgroups

Our analysis suggests that slope, accessibility, and department all explain differences in impact on forest cover across PLAs. We found that the highest ATT comes from PLAs between 20 and 25% slope (2.9% CIs +/- 1%) and that the average slope value for treated parcels is 20.4%. This suggests that the Colombian PLA network is well situated to take advantage of either the avoided deforestation or regrowth that occurs disproportionately on moderate slopes. For travel time, we found similar agreement between subgroups with the largest impact (0-2 hrs and 2-4 hrs) and the distribution of PLAs. Significant differences in impact across departments suggests that unobserved covariates likely influence PLA's impact on forest cover. Future work aimed at understanding these differences should consider both observed covariates at the department level as well as the unique socioeconomic and political dynamics of individual departments. Protection status subgroup results are ambiguous because only a small subset of PLAs fall inside a park or indigenous reserve; but our results suggest that PLAs inside other PAs may have a smaller impact on forest cover. Regardless of their impact, practitioners may still consider expanding PLAs into PAs as a social corrective for the uncompensated loss of land use rights that can accompany PAs in a region with high land tenure informality.

1.4.2. Cost Effectiveness

While this analysis is an important first step towards answering the question of where PLAs should be located, future work should estimate the cost-effectiveness for PLA subgroups before specific recommendations can be made. For example, if remote parcels have a relatively small impact on forest cover but are less expensive to protect, decision-makers might opt for protecting larger areas in remote parts of the country. This strategy could be particularly effective in dynamic landscapes like the Colombian Andes where deforestation pressure may expand alongside rural electrification or improved road networks (Garces et al., 2021). We also found that treatment effect increases over time and that the impact of PLAs on forest cover might not be immediately observable. Given this dynamic, we encourage researchers and decision-makers to reassess the impact of PLAs as the network expands and matures.

1.4.3. Regrowth vs. Avoided Deforestation

Previous work in Eastern Antioquia suggests that a large part of the impact PLAs have on forest cover is from regrowth as opposed to avoided deforestation (Reboredo Segovia et al., 2022). Because new or restored forests may not provide the same ecological value in terms of habitat or species richness, a top priority for future work should be to reproduce the analysis done in Eastern Antioquia for the full PLA dataset. To do this, ATT should be calculated based on products that either exclude forest gain or model forest loss explicitly (Hansen, 2013). Other future work includes reporting impact in hectares as opposed to percentages, estimating cost-effectiveness, and improving matching by incorporating deforestation pressure and spillover effects from nearby protection.

1.5. Conclusions

Colombia's unique legal structure requiring municipalities to spend 1% of their annual income on land acquisitions for water conservation presents a unique opportunity to study PLAs over a relatively long time period. We find that overall, PLAs have had a statistically significant positive impact on forest cover—3.5% (CIs +/- 1.2%) as of 2021—and that that the impact increases for several years post-treatment. Subgroup analysis reveals that impact on forest cover varies significantly by factors like slope and accessibility as well as geographically by department. Given these initial findings, we suggest future work that will quantify impact in more meaningful terms (area estimates, and cost effectiveness) and help characterize impact as either the result of avoided deforestation or forest regrowth. It is our hope that understanding PLA impacts in the data-rich Colombian context can help inform decision-makers as they attempt to build equitable and effective conservation networks in the face of global change.

1.6. References

Callaway, B., & Sant'Anna, P. H. C. (2021). Difference-in-differences with multiple time periods. Journal of Econometrics, 225, 200–230.

CEPF. (2015). Ecosystem Profile: Tropical Andes Biodiversity Hotspot. Arlington, VA.

Few, R., Ramírez, V., Armijos, M. T., Hernández, L. A. Z., & Marsh, H. (2021). Moving with risk: Forced displacement and vulnerability to hazards in Colombia. World Development, 144, 105482. https://doi.org/10.1016/j.worlddev.2021.105482

Fondo Acción, Fundepúblico y WCS. (2017). Artículo 111, Ley 99 de 1993. Bogotá, D.C.

Garces, E., Tomei, J., Franco, C. J., & Dyner, I. (2021). Lessons from last mile electrification in Colombia: Examining the policy framework and outcomes for sustainability. Energy Research & Social Science, 79, 102156. https://doi.org/10.1016/j.erss.2021.102156

Hansen, M. C. C., et al. (2013). High-resolution global maps of 21st-century forest cover change. Science, 342(6158), 850–853.

Healey, S. P., et al. (2018). Mapping forest change using stacked generalization: An ensemble approach. Remote Sensing of Environment, 204, 717–728.

Japan Aerospace Exploration Agency (2021). ALOS World 3D 30 meter DEM. V3.2, Jan 2021. Distributed by OpenTopography. https://doi.org/10.5069/G94M92HB. Accessed: 2024-03-31

Kennedy, R. E., et al. (2014). Bringing an ecological view of change to Landsat-based remote sensing. Frontiers in Ecology and the Environment, 12(6), 339–346.

Nelson, A. (2008) Estimated travel time to the nearest city of 50,000 or more people in year 2000. Global Environment Monitoring Unit - Joint Research Centre of the European Commission, Ispra Italy.

Nolte, C., Meyer, S. R., Sims, K. R. E., & Thompson, J. R. (2019). Voluntary, permanent land protection reduces forest loss and development in a rural-urban landscape. Conservation Letters, 1-9(9).

Olson, D. M., Dinerstein, E., Wikramanayake, E. D., Burgess, N. D., Powell, G. V. N., Underwood, E. C., D'amico, J. A., Itoua, I., Strand, H. E., Morrison, J. C., Loucks, C. J., Allnutt, T. F., Ricketts, T. H., Kura, Y., Lamoreux, J. F., Wettengel, W. W., Hedao, P., & Kassem, K. R. (2001). Terrestrial Ecoregions of the World: A New Map of Life on Earth. BioScience, 51(11), 933. https://doi.org/10.1641/0006-3568(2001)051[0933:teotwa]2.0.co;2

Reboredo, Ana L, et al. "Implementing Land Acquisitions for Watershed Services in the Tropical Colombian Andes Produces Marginal Progress for Advancing Area-

Based Conservation Objectives." Conservation Letters, vol. 16, no. 2, 22 Dec. 2022, https://doi.org/10.1111/conl.12932.

Ritchie, H., (2021) "Deforestation and Forest Loss" Published online at OurWorldInData.org. Retrieved from: 'https://ourworldindata.org/deforestation'

Small, C., Elvidge, C. D., Balk, D., & Montgomery, M. (2011). Spatial scaling of stable night lights. Remote Sensing of Environment, 115(2), 269–280. https://doi.org/10.1016/j.rse.2010.08.021

Waldron, A., et al. "Targeting Global Conservation Funding to Limit Immediate Biodiversity Declines." Proceedings of the National Academy of Sciences, vol. 110, no. 29, 1 July 2013, pp. 12144–12148, www.pnas.org/content/pnas/suppl/2013/06/26/1221370110.DCSupplemental/sapp.pdf, https://doi.org/10.1073/pnas.1221370110.

Zhu, Z., & Woodcock, C. E. (2014). Continuous change detection and classification of land cover using all available Landsat data. Remote Sensing of Environment, 144, 152–171.

CHAPTER 2: Improved Forest Change Mapping with SAR and CCDC in the Topographically-Complex Colombian Andes

Authors: Emily D. French, Paulo Arévalo

2.1. Introduction

Over the last several decades, advances in satellite remote sensing data acquisition and availability have led to a proliferation of methods and algorithms that can be used to monitor forest change from space. Historically, forest change monitoring has relied on optical sensors like Landsat and, since 2015, Sentinel-2. When used together, these sensors can provide observations with a 30 m spatial resolution as frequently as every two or three days allowing for detailed mapping and even near-real-time monitoring of forest disturbances. Unfortunately, optical sensors have one significant limitation—cloud cover. This is particularly problematic in regions like the Colombian Andes where cloud cover is so persistent that it precludes the use of optical data almost entirely. Over the last 10 years, synthetic aperture radar (SAR) data which at longer wavelengths are largely unaffected by clouds, have been introduced as a way to complement or even replace optical data in cases where the number of usable optical observations is insufficient.

The first SAR-based maps of annual global forest cover were produced in 2014 from ALOS PALSAR observations (Shimada et al., 2014). Since then, advances in SAR pre-processing and the integration of Sentinel-1 SAR data with Google Earth Engine (GEE) have allowed researchers to generate increasingly sophisticated forest change products from SAR data. Observations from Sentinel-1 have been particularly popular in efforts to build near real-time monitoring pipelines because of their 10 m spatial

resolution and reliable six day repeat cycle. Notably, the Radar for Detecting Deforestation (RADD) alert system uses Sentinel-1 observations to flag forest disturbances based on disturbance probabilities generated using historical backscatter values (Reiche et al., 2021). In 2022, Bullock et al., published the first application of SAR data with the Continuous Change Detection and Classification (CCDC) algorithm (Bullock et al., 2022). Given its ability to represent seasonality, disturbances, and trends, CCDC has become one of the most popular algorithms for land cover mapping and change detection (Zhu & Woodcock, 2014). While Bullock et al., focus on the use of CCDC with SAR data as a way to improve timeliness in forest change monitoring, this work explores whether CCDC can be used with SAR data to identify forest change in topographically complex landscapes.

One of the primary challenges when working with SAR observations is that radar backscatter is highly dependent on the interaction between terrain and radar geometry. As a result, most research using SAR data to map forest change has been done in areas of the tropics with relatively mild terrain features like Madagascar or the Congo Basin (Bullock et al., 2022; Reiche et al., 2021). Our study area, the Colombian Andes, is one of the most topographically complex parts of the world. It is also an incredibly biodiverse region with the largest variety of amphibians, birds, and mammals. Forests in this region provide key ecosystem services including carbon sequestration and water source protection. At the same time, this region experiences high rates of forest degradation and deforestation and ranks as one of the most threatened areas of the tropics (Ritchie, 2021; CEPF, 2015). In this context, decision makers are in need of detailed forest change information to help

inform land use planning and conservation efforts. In response to this need and the lack of usable optical data we ask: Can CCDC be used with SAR data to detect forest change in topographically complex regions like the Colombian Andes? We present our findings as both CCDC model breaks and land cover classifications generated by training a random forests model on CCDC coefficients.

2.2. Methods

2.2.1. Study Area

Ultimately, one of the goals of this research to help fill gaps in an optical ensemble model that predicts forest cover annually using Landsat observations. The existing model uses a stacking generalization protocol (Healey et al. 2018) to combine results from CCDC and LandTrendr with the Hansen global forest cover maps (Zhu & Woodcock, 2014; Kennedy et al., 2014; Hansen et al., 2013). Because the current ensemble model relies on Landsat data, we define our study area as any pixel that has fewer than 30 cloud-free Landsat observations between 1997 and 2021 (Figure 2.1). Going forward, we refer to this as the radar area since it represents any area where SAR data is needed to fill gaps in the existing optical ensemble model.

2.2.2. Sentinel-1 Data

This study uses Sentinel-1 Interferometric Wide (IW) swath mode Ground Range Detected (GRD) data accessed through GEE from 2017 to 2023 (Gorelick et al., 2017). The Sentinel-1 constellation has been collecting C-band dual polarization backscatter

data since 2014; however, timeseries over Colombia are not dense enough to use with CCDC until 2017. Sentinel-1 scenes available on GEE have already been pre-processed with the Sentinel-1 Toolbox. This includes GRD border noise removal, thermal noise removal, radiometric calibration to retrieve backscatter intensity, and orthorectification. The final units represent backscatter coefficient in decibels where negative values correspond to preferential scattering away from the SAR sensor and positive values represent preferential scattering towards the SAR sensor.

Sentinel-1 data are collected from both ascending and descending orbits. While view angle varies even among data from the same orbital direction, view angle variation is particularly pronounced among data obtained from different orbital directions. This is important because backscatter values are dependent on SAR view angle. Differences are further magnified over uneven terrain because of the interaction between topography and view angle. To minimize variation introduced by view angle as opposed to land cover change, we use data from the descending orbit only because descending observations are more common in our study area.

2.2.3. Study Period

Data acquisition varies considerably across the study area which, in some cases, results in data gaps of up to two months. While theoretically CCDC should be able to incorporate data gaps, early CDCC runs showed that erroneous breaks were frequently introduced after gaps greater than two months. To reduce uncertainty associated with these gaps, we ran CCDC with distinct start and end dates for four acquisition groups.

Groups were defined for areas with the same acquisition pattern based on the longest consecutive timeseries with acquisition gaps no longer than two months. Regardless of their start and end dates, all acquisition groups cover the three-year period between 2019 and the end of 2021. For simplicity, we present CCDC model breaks and timeseries for examples from the two largest groups which run from April, 2017 to November, 2023 and October, 2018 to November, 2023 and land cover classification results based on CCDC coefficients from 2020.

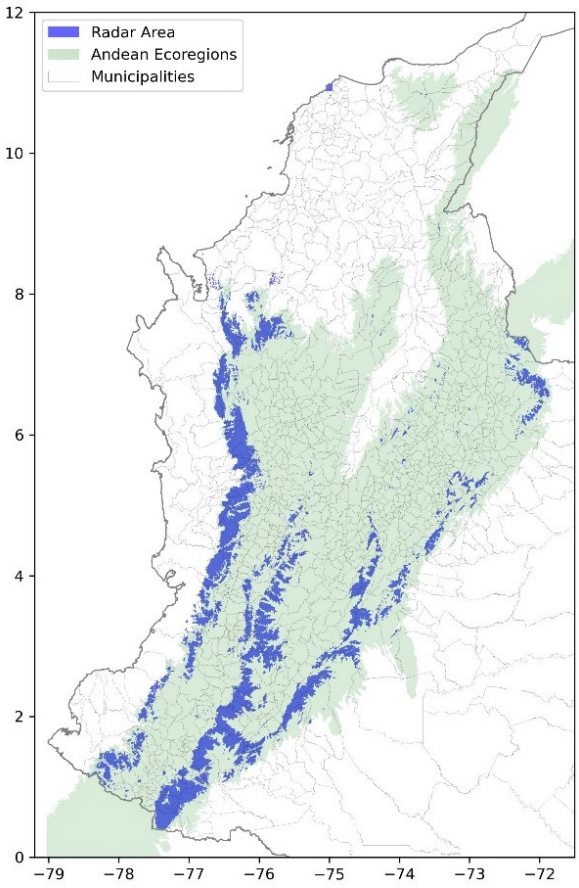

Figure 2.1. Study area including areas with fewer than 30 Landsat observations (blue) and Andean Ecoregions (green) including Northern Andean Montane Forests, Northern Andean Parámo, and Tumbesian-Andean Valleys Dry Forests (Olson et al., 2001).

2.2.4. SAR pre-processing

Based on Sentinel-1 pre-processing recommendations outlined in Bullock et al. (2022), we used a simple spatial mean filter to further reduce speckle followed by the Refined Lee Filter (Yommy et al., 2015), and radiometric terrain correction (Vollrath et al., 2020). Radiometric terrain correction (RTC) is necessary because radiometric distortions over complex terrain are large enough to mask the weaker signal from land cover variation. Importantly, the model developed by Vollrath et al., provides a mask for active layover and shadow areas where change detection would be impossible. Finally, we calculated a ratio index between VV and VH polarization bands which allows for RGB visualizations (Figure 2.2).

2.2.5. Continuous Change Detection and Classification (CCDC)

Continuous Change Detection and Classification (CCDC) is a temporal segmentation algorithm that was originally developed for use with Landsat timeseries (Zhu & Woodcock, 2014). One of the primary strengths of CCDC is that it provides information about seasonality, abrupt change (eg. deforestation), and gradual change (eg. forest regrowth or degredation). CCDC works by fitting a model to observations and then evaluating predicted values against new observations. When the residual of predicted and observed values exceeds a probability threshold multiple times, a change is detected. These changes are often referred to as breaks. In this study, we flagged change when 6 observations exceeded a chi-squared probability value of 0.99. We used VV, VH, and the ratio between VV and VH bands as CCDC inputs. Since forested areas have high VH

backscatter, we primarily used VH band breaks to identify areas of potential deforestation. Another strength of CCDC is that because it requires multiple observations to trigger a break, it is not sensitive to single anomalous observations like clouds in optical data or atmospheric propagation effects which sometimes appear in C-band radar data (Danklmayer et al., 2009).

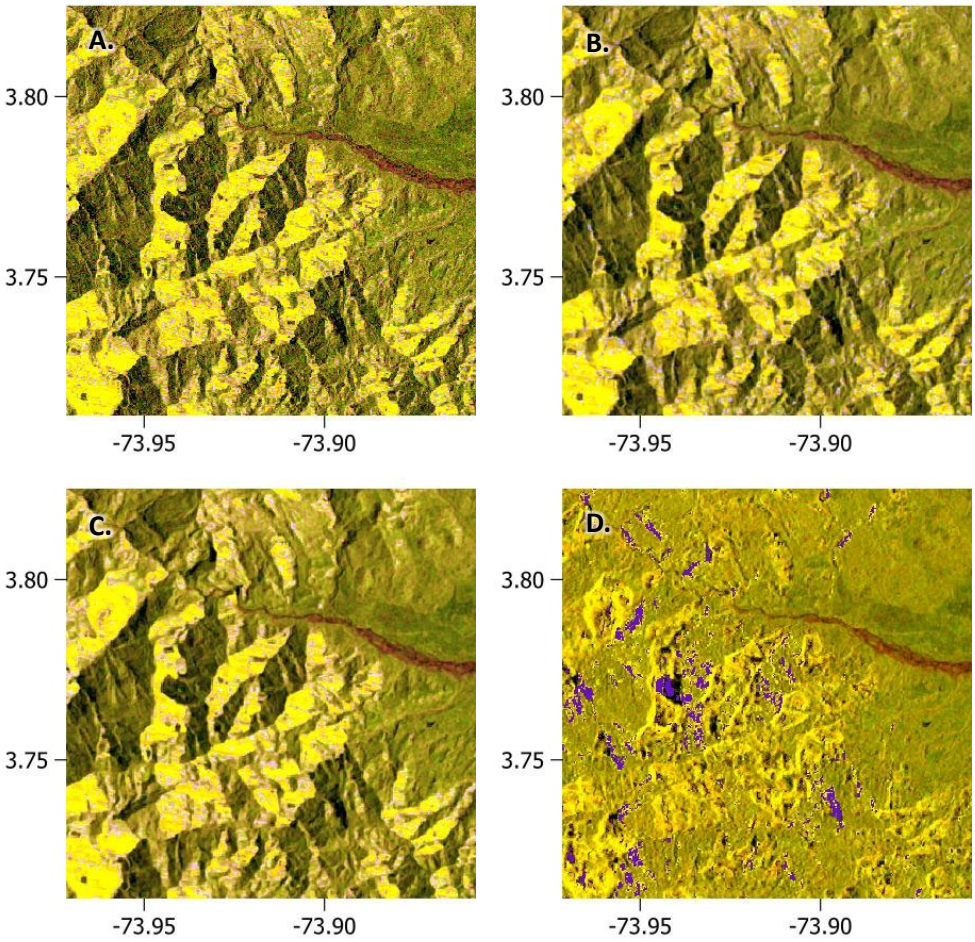

Figure 2.2. RGB visualization of the VV, VH, and ratio bands for a Sentinel-1 image with no additional pre-processing (a); simple spatial mean (b); simple spatial mean and refined lee filter (c); and simple spatial mean, refined lee, and radiometric terrain correction where purple highlights radar layover or shadow areas that have been masked by the radiometric terrain correction.

2.2.6. Random Forests Land Cover Classification

To assess and classify CCDC outputs, we adapted code developed by Arévalo et al. (2020) for working with Landsat CCDC outputs in GEE. Instead of manually compiling a training dataset, we took advantage of the existing land cover maps generated by the optical ensemble model described above. To do this, we drew a stratified random sample from a 2km buffer around the radar area where we know the ensemble has enough Landsat observations to predict land cover with a high degree of accuracy (accuracy assessment in progress). Sampled classes include: forest, herbaceous, developed, barren, and water. Previous work shows that random forest classifiers are sensitive to the class proportions of training data (Zhu et al., 2016). Given these findings, we drew training points so that the number of points per class is roughly proportional to the expected land cover area. We then trained a random forests classifier on CCDC coefficients and terrain information. The best classification (based on visual assessment) included the amplitude, intercept, RMSE, phase, and slope for VV and VH bands and aspect.

2.3. Results & Discussion

2.3.1. Results

This work is the first attempt to detect forest change using SAR and CCDC in a region as topographically complex as the Colombian Andes. We find that observations from 24.6% of our study area are unusable due to radar shadow or layover. Despite this limitation, we find encouraging evidence to suggest that CCDC can be used with SAR

data to detect forest change in difficult terrain. VH band model breaks correspond both spatially and temporally with visible deforestation in high-resolution Planet basemaps (Figure 2.3, Figure 2.4); though we observe a strong correlation between missed deforestation and aspect which suggests that results would be improved by combining separate CCDC runs for ascending and descending orbits wherever possible. We also observe landscape-level spatial coherence between classification results and land cover (Figure 2.5).

While initial results are encouraging, both CCDC breaks and classification results are visibly noisy—particularly in steep terrain (Figure 2.6). While some of this noise can be filtered after running CCDC or even after classification, aggressive post-processing runs the risk of eliminating small but valid change areas. In this context, we dedicate the rest of this chapter to a discussion about potential SAR pre-processing improvements.

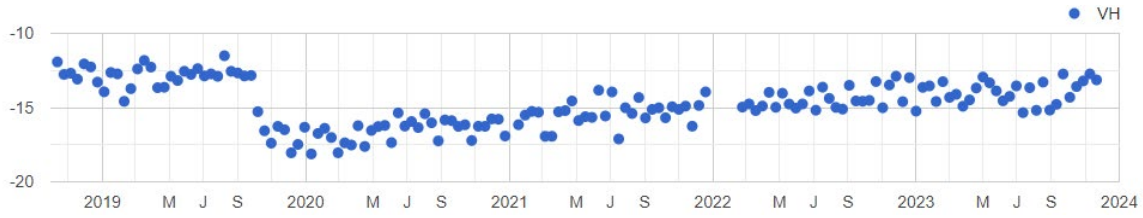

Figure 2.3. VH Timeseries showing a decrease in backscatter corresponding to deforestation in late 2019.

2.3.2. Radiometric Terrain Correction Limitations

The radiometric terrain correction (RTC) used for this study has several limitations. First, the quality of the correction is entirely dependent on the underlying terrain geometry provided by the DEM. Errors will inevitably be introduced if the spatial

resolution of the DEM is larger than the input data and in places where the surface has changed between DEM and scene acquisitions. For example, we use a 30 m DEM to correct 10 m Sentinel-1 pixels and find pervasive 30 m artifacts in our 10 m results, especially in areas with steep slopes where imprecise terrain data are expected to have a large impact. Given that there is currently no freely available 10 m DEM for Colombia, this is a limitation that we may not be able to address. If possible, we hope to incorporate a 12m TanDEM-X DEM available to researchers through a proposal process in future iterations of this research. To minimize the potential for error introduced by surface changes, we uploaded a freely available 30m DEM acquired in 2015 by the German Aerospace Center's TanDEM-X satellite instead of using SRTM which was already available on GEE but is based on observations that were acquired in 2000. We encourage other researchers to choose a DEM that matches the spatial resolution and acquisition date of their observations as closely as possible.

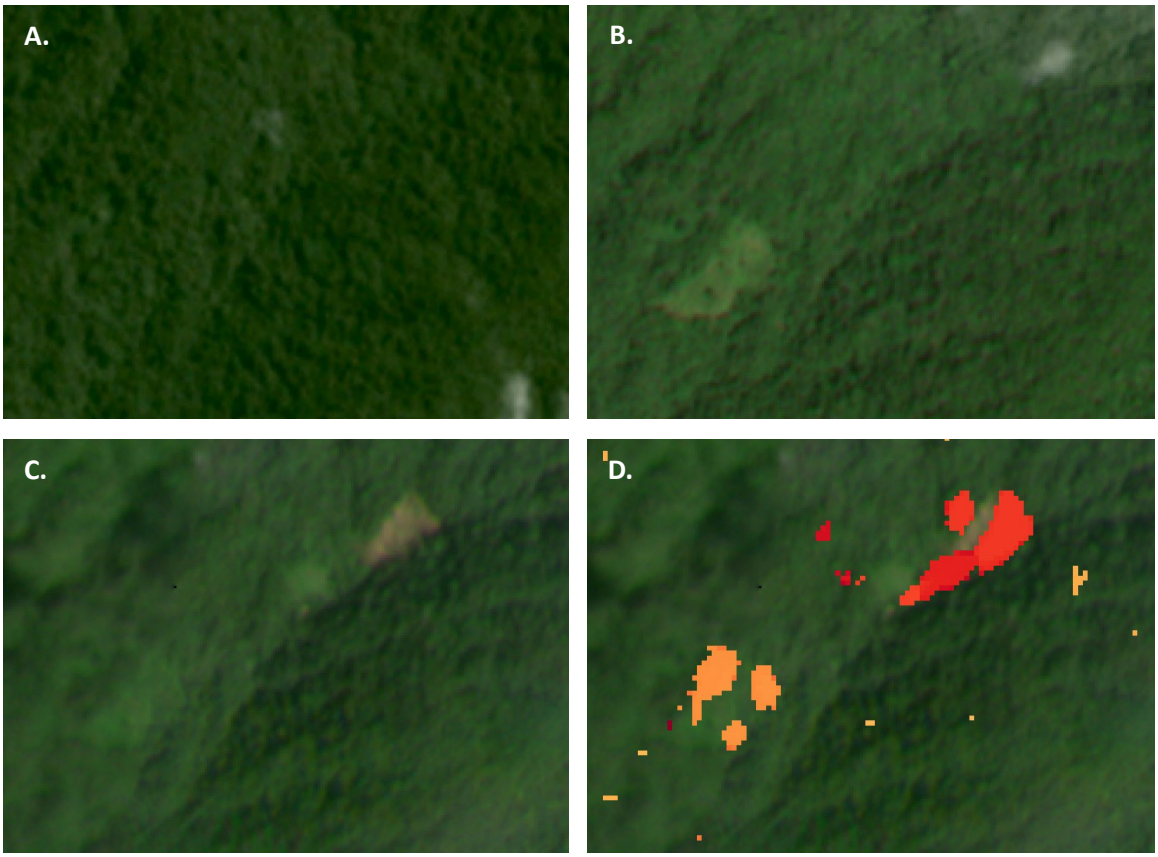

Figure 2.4. Planet basemaps from 2016 (a); 2019 (b); and 2020 (c); CCDC model breaks (d) correspond to deforestation in 2019 (orange) and 2020 (red).

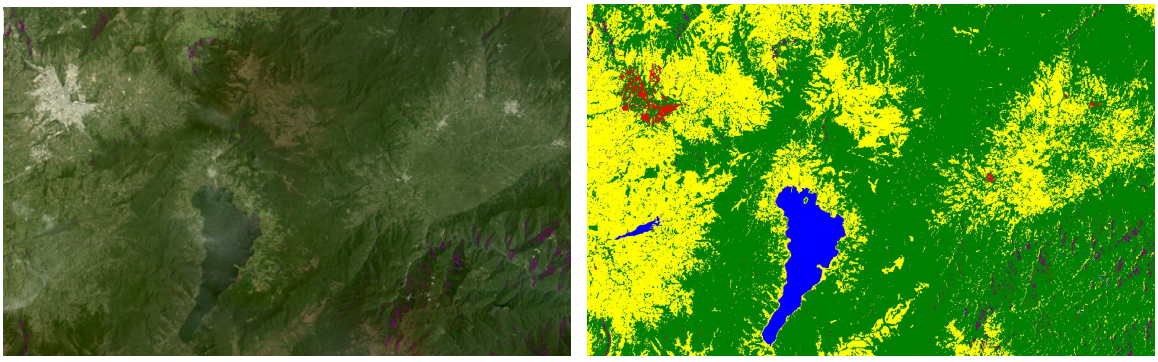

Figure 2.5. Landscape-level spatial coherence between Planet basemap from December, 2019 (a) and CCDC coefficient classification results for 2020 (b) near Pasto, Colombia. Landcover classes include forest (green), herbaceous (yellow), developed (red), barren (grey) and water (blue). Radar layover and shadow areas shown in purple on both images.

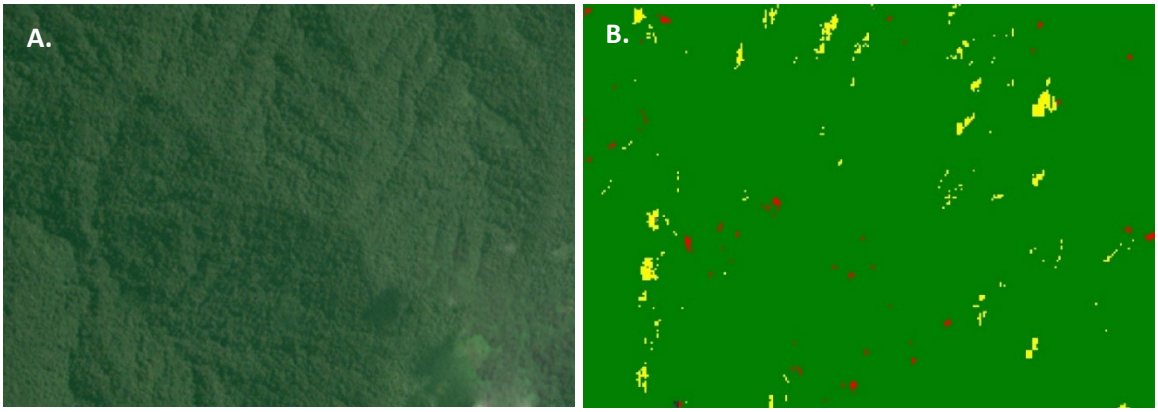

Figure 2.6. Planet basemap for June, 2020 (a) and noisy CCDC coefficient classification results for 2020 (b).

A second limitation of the radiometric terrain correction is that it requires users to pick between two models—a volume scattering model optimized for vegetated areas and a surface scattering model optimized for built environments. Given that our primary goal is to identify forest change, we used the volume scattering model, but we recognize that this may limit the accuracy of classification results in heterogenous landscapes. Future work could investigate if classification results can be improved by training a random forests model on CCDC coefficients from two separate CCDC runs each based on different scattering model.

Another significant limitation of the radiometric terrain correction we implemented in GEE (Vollrath et al., 2020) is that it makes a simplified assumption that pixel area is constant across a Sentinel-1 scene when in reality, pixel area varies based on terrain variations. This assumption is necessary because information about the satellite's positional state vectors is left out when Sentinel-1 data are ingested into the GEE data catalogue; (Vollrath, 2024) but, results in a simplified model where pixel-to-pixel correspondence is assumed between Sentinel-1 scenes and the DEM. A recent study

comparing open-source RTC software highlights this limitation and shows that RTC in GEE performs much less effectively in steep terrain compared to standalone software packages that use pixel area correction (Flores-Anderson et al., 2023). These findings support our observation that RTC errors are the primary cause of noise and artifacts in our results and suggest that, at present, it may not be possible to run CCDC with SAR data using GEE exclusively (Figure 2.7). Future work should explore the feasibility of uploading locally generated pixel areas bands to GEE and incorporating them into existing RTC GEE code. It should also include a formal accuracy assessment so that improvements can be measured objectively instead of by visual assessment alone.

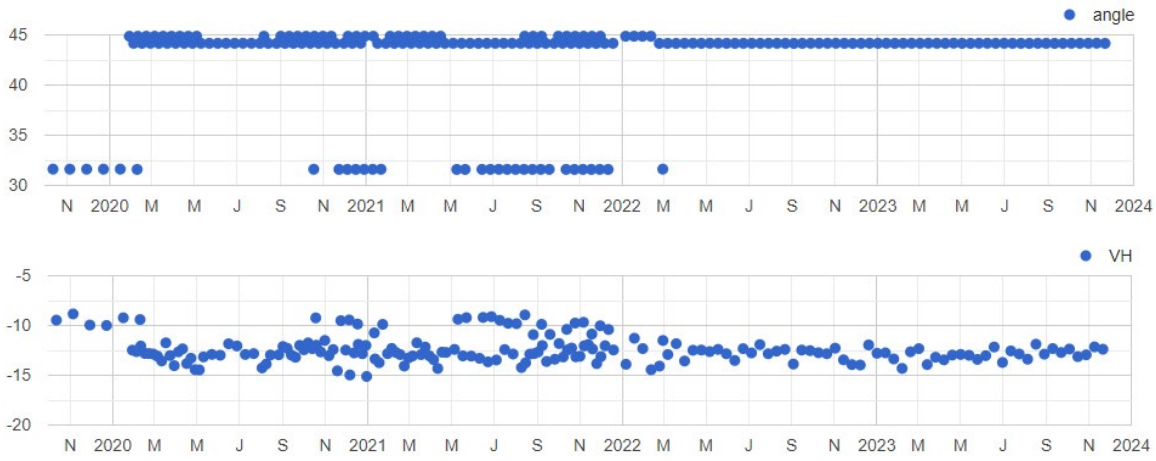

Figure 2.7. Correspondence between incidence angle (top), and VH backscatter values (bottom) for a pixel with no observable land use change.

2.4. Conclusions

Given the potential for SAR data to help us better understand forest change dynamics in cloudy areas like the Colombian Andes, we investigate whether CCDC can be used with Sentinel-1 data to detect forest change in topographically complex regions. We find that observations from a large portion of our study area, 24.6%, are unusable due

to radar layover and shadow. This area could be reduced by using data from both orbital directions; though in our study area, improvements may be minimal given the limited number of ascending observations. Encouragingly, CCDC breaks in the VH band correspond spatially and temporally with observed deforestation in high-resolution Planet imagery. We also observe spatial coherence between classification results from a random forests model trained on CCDC coefficients and landscape-level land cover. Ultimately, we conclude that CCDC can be used with SAR data to detect forest change in topographically-complex landscapes, but that accuracy improvements and widespread adoption of SAR workflows are dependent on the accessibility of high-resolution DEMs and improving radiometric terrain correction in GEE.

2.5. References

Arévalo, P., Bullock, E. L., Woodcock, C. E., & Olofsson, P. (2020). A Suite of Tools for Continuous Land Change Monitoring in Google Earth Engine. Frontiers in Climate, 2. https://doi.org/10.3389/fclim.2020.576740

Bullock, E. L., Healey, S. P., Yang, Z., Houborg, R., Gorelick, N., Tang, X., & Andrianirina, C. (2022). Timeliness in forest change monitoring: A new assessment framework demonstrated using Sentinel-1 and a continuous change detection algorithm. Remote Sensing of Environment, 276, 113043. https://doi.org/10.1016/j.rse.2022.113043

CEPF. (2015). Ecosystem Profile: Tropical Andes Biodiversity Hotspot. Arlington, VA.

Danklmayer A, Doring B, Schwerdt M and Chandra M. (2009) Assessment of Atmospheric Propagation Effects in SAR Images Assessment of Atmospheric Propagation Effects in SAR Images IEEE Trans. Geosci. Remote Sensing 47 3507–18

Flores-Anderson, A. I., Parache, H. B., Martin-Arias, V., Jiménez, S. A., Herndon, K., Mehlich, S., Meyer, F. J., Agarwal, S., Ilyushchenko, S., Agarwal, M., Nicolau, A., Markert, A., Saah, D., & Cherrington, E. (2023). Evaluating SAR Radiometric Terrain Correction Products: Analysis-Ready Data for Users. Remote Sensing, 15(21), 5110. https://doi.org/10.3390/rs15215110

Gorelick, N., Hancher, M., Dixon, M., Ilyushchenko, S., Thau, D., & Moore, R. (2017). Google Earth Engine: Planetary-scale geospatial analysis for everyone. Remote Sensing of Environment, 202, 18–27. https://doi.org/10.1016/j.rse.2017.06.031

Herold, M., 2021. Forest disturbance alerts for the Congo Basin using Sentinel-1. Environ. Res. Lett. https://doi.org/10.1088/1748-9326/abd0a8.

Hoekman D., Hand Reiche J., 2015. Multi-model radiometric slope correction of SAR images of complex terrain using a two-stage semi-empirical approach Remote Sens. Environ. 156 1–10

Olson, D. M., Dinerstein, E., Wikramanayake, E. D., Burgess, N. D., Powell, G. V. N., Underwood, E. C., D'amico, J. A., Itoua, I., Strand, H. E., Morrison, J. C., Loucks, C. J., Allnutt, T. F., Ricketts, T. H., Kura, Y., Lamoreux, J. F., Wettengel, W. W., Hedao, P., & Kassem, K. R. (2001). Terrestrial Ecoregions of the World: A New Map of Life on Earth. BioScience, 51(11), 933. https://doi.org/10.1641/0006-3568(2001)051[0933:teotwa]2.0.co;2

Quegan S and YuJ J 2001 Filtering of multichannel SAR images IEEE Trans. Geosci. Remote Sens. 39 2373–9

Reiche, J., Mullissa, A., Slagter, B., Gou, Y., Tsendbazar, N.-E., Odongo-Braun, C., Vollrath, A., Weisse, M. J., Stolle, F., Pickens, A., Donchyts, G., Clinton, N., Gorelick, N., & Herold, M. (2021). Forest disturbance alerts for the Congo Basin using Sentinel-1. Environmental Research Letters, 16(2), 024005. https://doi.org/10.1088/1748-9326/abd0a8

Ritchie, H. (2021). "Deforestation and Forest Loss" Published online at OurWorldInData.org. Retrieved from: 'https://ourworldindata.org/deforestation'

Shimada, M., Itoh, T., Motooka, T., Watanabe, M., Shiraishi, T., Thapa, R., & Lucas, R. (2014). New global forest/non-forest maps from ALOS PALSAR data (2007–2010). Remote Sensing of Environment, 155, 13–31. https://doi.org/10.1016/j.rse.2014.04.014

Vollrath, A. (2024). Improved Sentinel-1 Analysis-Ready-Data on Google's Earth Engine. https://www.linkedin.com/pulse/improved-sentinel-1-analysis-ready-data-googles-earth-vollrath-gdine/?trackingId=qi4vlVX9JL%2BE1d5pmYpK3A%3D%3D

Vollrath, A., Mullissa, A., & Reiche, J. (2020). Angular-Based Radiometric Slope Correction for Sentinel-1 on Google Earth Engine. Remote Sensing, 12(11), 1867. https://doi.org/10.3390/rs12111867

Yommy, Aiyeola & Liu, Rongke & Wu, And. (2015). SAR Image Despeckling Using Refined Lee Filter. 260-265. https://doi.org/10.1109/IHMSC.2015.236

Zhu, Z., Gallant, A.L., Woodcock, C.E., Pengra, B., Olofsson, P., Loveland, T.R., Jin, S., Dahal, D., Yang, L., and R.F. Auch, 2016. Optimizing selection of training and auxiliary data for operational land cover classification for the LCMAP initiative. ISPRS Journal of Photogrammetry and Remote Sensing (122):206-221.

Zhu, Z., & Woodcock, C. E. (2014). Continuous change detection and classification of land cover using all available Landsat data. Remote Sensing of Environment, 144, 152–171. https://doi.org/10.1016/j.rse.2014.01.011

CUMULATIVE REFERENCES

Arévalo, P., Bullock, E. L., Woodcock, C. E., & Olofsson, P. (2020). A Suite of Tools for Continuous Land Change Monitoring in Google Earth Engine. *Frontiers in Climate*, 2, 576740. https://doi.org/10.3389/fclim.2020.576740

Bullock, E. L., Healey, S. P., Yang, Z., Houborg, R., Gorelick, N., Tang, X., & Andrianirina, C. (2022). Timeliness in forest change monitoring: A new assessment framework demonstrated using Sentinel-1 and a continuous change detection algorithm. *Remote Sensing of Environment*, 276, 113043. https://doi.org/10.1016/j.rse.2022.113043

Callaway, B., & Sant'Anna, P. H. C. (2021). Difference-in-differences with multiple time periods. *Journal of Econometrics*, 225, 200–230. https://doi.org/10.1016/j.jeconom.2020.12.001

CEPF. (Critical Ecosystem Partnership Fund) (2015). Ecosystem Profile: Tropical Andes Biodiversity Hotspot. Arlington, VA.

Danklmayer A., Doring B., Schwerdt M. & Chandra M. (2009) Assessment of Atmospheric Propagation Effects in SAR Images. *IEEE Transactions on Geoscience and Remote Sensing,* 47(10), 3507–3518. https://doi.org/10.1109/TGRS.2009.2022271

Few, R., Ramírez, V., Armijos, M. T., Hernández, L. A. Z., & Marsh, H. (2021). Moving with risk: Forced displacement and vulnerability to hazards in Colombia. *World Development*, 144, 105482. https://doi.org/10.1016/j.worlddev.2021.105482

Flores-Anderson, A.I., Parache, H. B., Martin-Arias, V., Jiménez, S. A., Herndon, K., Mehlich, S., Meyer, F. J., Agarwal, S., Ilyushchenko, S., Agarwal, M., Nicolau, A., Markert, A., Saah, D., & Cherrington, E. (2023). Evaluating SAR Radiometric Terrain Correction Products: Analysis-Ready Data for Users. *Remote Sensing*, 15(21), 5110. https://doi.org/10.3390/rs15215110

Fondo Acción, Fundepúblico y WCS. (2017). Artículo 111, Ley 99 de 1993. Bogotá, D.C. https://colombia.wcs.org/Portals/113/Noticias/Negocios%20y%20biodiversidad/Cartilla-arti%CC%81culo-111.pdf

Garces, E., Tomei, J., Franco, C. J., & Dyner, I. (2021). Lessons from last mile electrification in Colombia: Examining the policy framework and outcomes for sustainability. *Energy Research & Social Science*, 79, 102156. https://doi.org/10.1016/j.erss.2021.102156

Gorelick, N., Hancher, M., Dixon, M., Ilyushchenko, S., Thau, D., & Moore, R. (2017). Google Earth Engine: Planetary-scale geospatial analysis for everyone. *Remote*

Sensing of Environment, 202, 18–27. https://doi.org/10.1016/j.rse.2017.06.031

Hansen, M. C. C., et al. (2013). High-resolution global maps of 21st-century forest cover change. *Science*, 342(6160), 850–853. https://doi.org/10.1126/science.1244693

Healey, S. P., et al. (2018). Mapping forest change using stacked generalization: An ensemble approach. *Remote Sensing of Environment*, 204, 717–728. https://doi.org/10.1016/j.rse.2017.09.029

Hoekman D., Hand Reiche J., 2015. Multi-model radiometric slope correction of SAR images of complex terrain using a two-stage semi-empirical approach. *Remote Sensing of Environment,* 156, 1–10. https://doi.org/10.1016/j.rse.2014.08.037

Japan Aerospace Exploration Agency (2021). ALOS World 3D 30 meter DEM. V3.2, Jan 2021. Distributed by OpenTopography. https://doi.org/10.5069/G94M92HB. Accessed: 2024-03-31

Kennedy, R. E., et al. (2014). Bringing an ecological view of change to Landsat-based remote sensing. *Frontiers in Ecology and the Environment*, 12(6), 339–346. https://doi.org/10.1890/130066

Nelson, A. (2008) Estimated travel time to the nearest city of 50,000 or more people in year 2000. Global Environment Monitoring Unit – Joint Research Centre of the European Commission, Ispra Italy. https://forobs.jrc.ec.europa.eu/data/products/gam/access_50k.zip

Nolte, C., Meyer, S. R., Sims, K. R. E., & Thompson, J. R. (2019). Voluntary, permanent land protection reduces forest loss and development in a rural-urban landscape. *Conservation Letters,* 12(6), e12649. https://doi.org/10.1111/conl.12649

Olson, D. M., Dinerstein, E., Wikramanayake, E. D., Burgess, N. D., Powell, G. V. N., Underwood, E. C., D'amico, J. A., Itoua, I., Strand, H. E., Morrison, J. C., Loucks, C. J., Allnutt, T. F., Ricketts, T. H., Kura, Y., Lamoreux, J. F., Wettengel, W. W., Hedao, P., & Kassem, K. R. (2001). Terrestrial Ecoregions of the World: A New Map of Life on Earth. *BioScience*, 51(11), 933–938. https://doi.org/10.1641/0006-3568(2001)051[0933:teotwa]2.0.co;2

Quegan S. & Yu, J.J. (2001). Filtering of multichannel SAR images. *IEEE Transactions on Geoscience and Remote Sensing,* 39, 2373–2379. https://doi.org/10.1109/36.964973

Reboredo Segovia, Ana L, et al. (2022). Implementing Land Acquisitions for Watershed Services in the Tropical Colombian Andes Produces Marginal Progress for Advancing Area-Based Conservation Objectives. *Conservation Letters*, 16(2), e12932. https://doi.org/10.1111/conl.12932.

Reiche, J., Mullissa, A., Slagter, B., Gou, Y., Tsendbazar, N.-E., Odongo-Braun, C., Vollrath, A., Weisse, M. J., Stolle, F., Pickens, A., Donchyts, G., Clinton, N., Gorelick, N., & Herold, M. (2021). Forest disturbance alerts for the Congo Basin using Sentinel-1. *Environmental Research Letters*, 16(2), 024005. https://doi.org/10.1088/1748-9326/abd0a8

Ritchie, H., (2021) "Deforestation and Forest Loss" Published online at OurWorldInData.org. Retrieved from: 'https://ourworldindata.org/deforestation'

Shimada, M., Itoh, T., Motooka, T., Watanabe, M., Shiraishi, T., Thapa, R., & Lucas, R. (2014). New global forest/non-forest maps from ALOS PALSAR data (2007–2010). *Remote Sensing of Environment*, 155, 13–31. https://doi.org/10.1016/j.rse.2014.04.014

Small, C., Elvidge, C. D., Balk, D.,& Montgomery, M. (2011). Spatial scaling of stable night lights. *Remote Sensing of Environment*, 115(2), 269–280. https://doi.org/10.1016/j.rse.2010.08.021

Vollrath, A. (2024). Improved Sentinel-1 Analysis-Ready-Data on Google's Earth Engine. https://www.linkedin.com/pulse/improved-sentinel-1-analysis-ready-data-googles-earth-vollrath-gdine/

Vollrath, A., Mullissa, A., & Reiche, J. (2020). Angular-Based Radiometric Slope Correction for Sentinel-1 on Google Earth Engine. *Remote Sensing*, 12(11), 1867. https://doi.org/10.3390/rs12111867

Waldron, A., et al. (2013). Targeting Global Conservation Funding to Limit Immediate Biodiversity Declines. *Proceedings of the National Academy of Sciences of the United States of America*, 110(29), 12144–12148, https://doi.org/10.1073/pnas.1221370110

Yommy, Aiyeola & Liu, Rongke & Wu, And. (2015). SAR Image Despeckling Using Refined Lee Filter. In *2015 7th International Conference on Intelligent Human-Machine Systems and Cybernetics*, pp. 260–265. https://doi.org/10.1109/IHMSC.2015.236

Zhu, Z., Gallant, A.L., Woodcock, C.E., Pengra, B., Olofsson, P., Loveland, T.R., Jin, S., Dahal, D., Yang, L., and R.F. Auch, 2016. Optimizing selection of training and auxiliary data for operational land cover classification for the LCMAP initiative. *ISPRS Journal of Photogrammetry and Remote Sensing*, 122, 206–221. https://doi.org/10.1016/j.isprsjprs.2016.11.004

Zhu, Z., & Woodcock, C. E. (2014). Continuous change detection and classification of land cover using all available Landsat data. *Remote Sensing of Environment*, 144, 152–171. https://doi.org/10.1016/j.rse.2014.01.011

CURRICULUM VITAE